Anthrax Protective Antigen: Prepore-to-Pore Conversion[†]

Carl J. Miller, Jennifer L. Elliott, and R. John Collier*

Department of Microbiology and Molecular Genetics, Harvard Medical School, 200 Longwood Avenue, Boston, Massachusetts 02115

Received April 6, 1999; Revised Manuscript Received June 3, 1999

ABSTRACT: PA_{63}, the active 63 kDa form of anthrax protective antigen, forms a heptameric ring-shaped oligomer that is believed to represent a precursor of the membrane pore formed by this protein. When maintained at pH ≥8.0, this "prepore" dissociated to monomeric subunits upon treatment with SDS at room temperature, but treatment at pH ≤7 (or with β-octylglucoside at pH 8.0) caused it to convert to an SDS-resistant pore-like form. Transition to this form involved major changes in the conformation of loop 2 of domain 2 (D2L2), as evidenced by (i) occlusion of a chymotrypsin site within D2L2 and (ii) excimer formation by pyrene groups linked to N306C within this loop. The pore-like form retained the capacity to bind anthrax toxin A moieties and cell surface receptors, but was unable to form pores in membranes or mediate translocation. Mutant PA_{63} in which D2L2 had been deleted was inactive in pore formation and translocation but, like the prepore, was capable of forming heptamers that converted to an SDS-resistant form under acidic conditions. Our findings support a model of pore formation in which the D2L2 loops move to the membrane-proximal face of the heptamer and interact to form a 14-strand transmembrane β-barrel. Concomitantly, domain 2 undergoes a major conformational rearrangement, independent of D2L2, that renders the heptamer resistant to dissociation by SDS. These results provide a basis for further exploration of the role of PA_{63} in translocation of anthrax toxin's enzymic moieties across membranes.

The process by which intracellularly acting toxins translocate their enzymic A moieties across membranes to gain access to substrates within the cytosol is not well understood. In some members of this class (such as diphtheria, tetanus, and anthrax toxins), the receptor-binding B moiety has the ability to insert into membranes and form aqueous pores (channels) under conditions known to promote translocation. This has led to speculation that such pores serve as passageways for translocation of the enzymic A moieties across membranes. Consistent with this hypothesis, mutations within the B moieties of diphtheria and anthrax toxins that block their ability to form pores have also been found to block translocation (*1*−*3*), implying that the pore (or a step in its formation) is essential for translocation. However, the precise relationship between pore formation and translocation has not yet been clearly defined for any toxin.

Anthrax toxin has emerged as a promising model for exploring such questions, in part because the A and B moieties are synthesized as discrete unassociated proteins and may be characterized separately (*4*). Recently, it has been possible to determine the X-ray crystallographic structure of the B moiety of anthrax toxin, protective antigen (PA),[1] and of a heptameric ring-shaped derivative of PA that is believed to represent a precursor of the pore formed by this protein (*5*). A detailed understanding of pore structure and function in this system is therefore coming within reach.

Anthrax toxin represents the prototypic example of so-called binary bacterial toxins. In such toxins, the A and B moieties self-assemble at the surface of mammalian cells to form noncovalent toxic complexes, which are then internalized and serve to deliver the A moiety to the cytosol (Figure 1). PA, a water-soluble 83 kDa protein, binds to a receptor that is present on most mammalian cells (*6*) and is then cleaved by furin or furin-like proteases into two fragments: PA_{63}, a 63 kDa C-terminal fragment, which remains receptor-bound; and PA_{20}, a 20 kDa N-terminal fragment, which is released into the medium (*7*). Dissociation of PA_{20} allows PA_{63} to bind either or both of the two alternative A moieties of the toxin: edema factor (EF) and lethal factor (LF). The resulting hetero-oligomeric complexes are then endocytosed and trafficked to an acidic intracellular compartment, where EF and LF are translocated across the bounding membrane to the cytosol in response to low pH (*8*, *9*). EF is a calmodulin-dependent adenylate cyclase, whose activity may protect the bacteria from destruction by phagocytes (*10*). LF is a metalloprotease that is capable of killing macrophages or, at lower concentrations, inducing these cells to overproduce cytokines that can cause death of the host (*11*).

[†] This work was supported by NIH Grant AI22021 (R.J.C.).

* To whom correspondence should be addressed: 200 Longwood Ave., Boston, MA 02115. Phone: (617) 432-1930. Fax: (617) 432-0115. E-mail: John_Collier@hms.harvard.edu.

[1] Abbreviations: AT, anthrax toxin; LF_n, 255 N-terminal residues of lethal factor; DTA, catalytic subunit of diphtheria toxin; EF, edema factor; LF, lethal factor; nPA, trypsin-nicked protective antigen; PA, protective antigen; PA_{63}, C-terminal 63 kDa fragment of PA; s-pore, solution-formed pore; m-pore, membrane-formed pore; PAGE, polyacrylamide gel electrophoresis; PBS, phosphate-buffered saline; D2L2, domain 2 of loop 2 (residues 302−325); β-OG, β-octylglucoside; DOC, sodium deoxycholate; PM, *N*-(1-pyrene)maleimide; DTT, dithiothreitol.

10.1021/bi990792d CCC: $18.00
Published on Web 07/22/1999

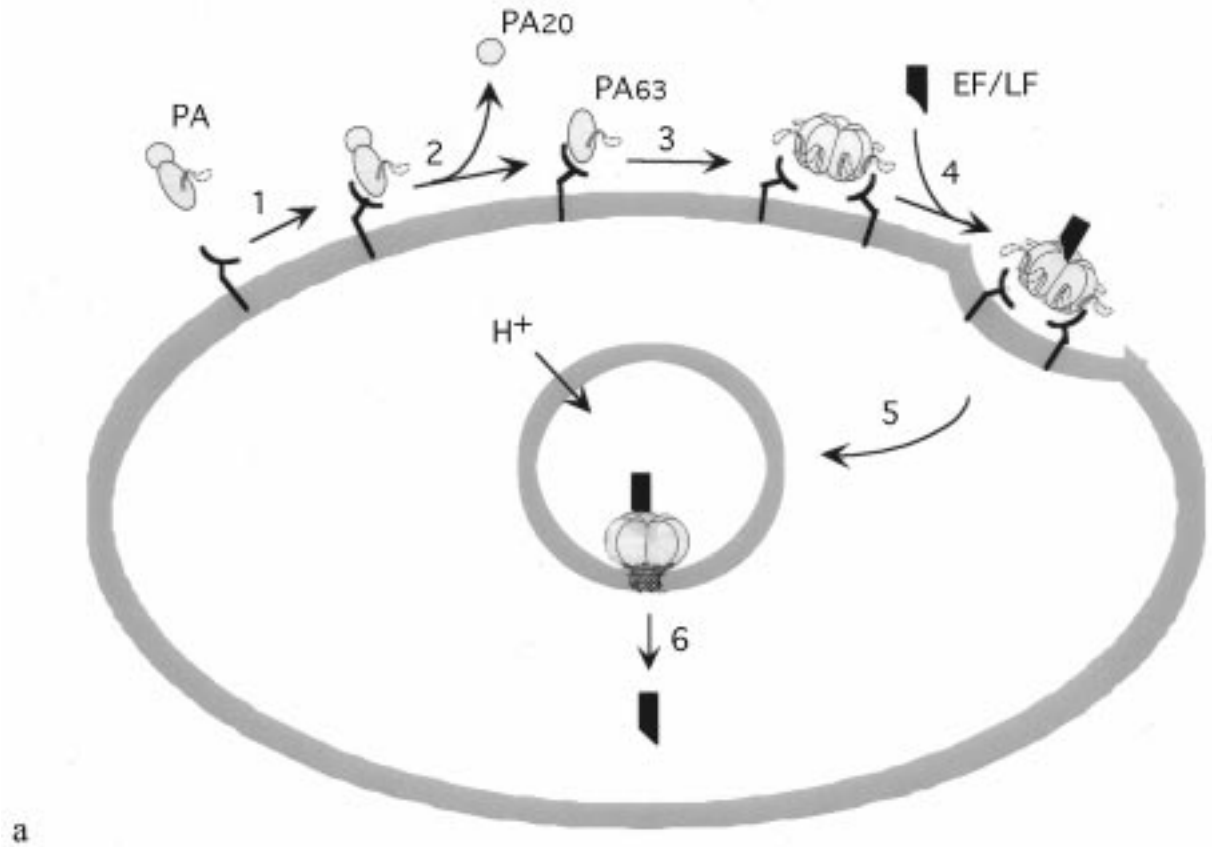

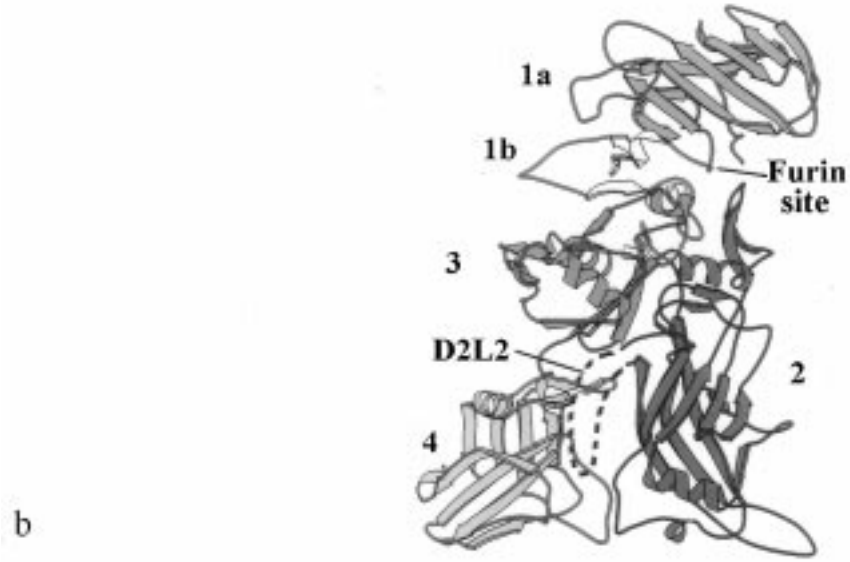

FIGURE 1: (a) Model of anthrax toxin entry into cells. (1) Binding of PA (loop being D2L2, residues 302−325) to its receptor. (2) Proteolytic activation of PA and dissociation of PA_{20}. (3) Self-association of monomeric PA_{63} to form the heptameric prepore. (4) Binding of EF/LF to the prepore. (5) Endocytosis of the receptor−PA_{63}−ligand complex. (6) pH-dependent conversion of the prepore to the pore, and translocation of the ligand to the cytosol. (b) Ribbon diagram of native protective antigen.

Besides enabling PA to bind EF and LF, proteolytic removal of PA_{20} also unveils PA's ability to insert into membranes and form pores (*12*). PA_{63} purified from trypsin-activated PA by anion-exchange chromatography has been shown to form cation-selective pores (channels) in planar lipid bilayers and to permeabilize liposomes and whole cells to monovalent cations (*13*, *14*). These activities are promoted by acidic pH, consistent with the known inhibition of anthrax toxin action by lysosomotropic agents. (The pH dependence of pore formation varies, depending on the nature of the membrane, as discussed below.) Neither PA nor PA_{20} exhibits pore forming activity.

Electron microscopy of negatively stained samples of PA_{63} revealed that the protein forms ring-shaped heptamers containing a central cavity (*12*). The possibility that these oligomers are relevant to pore formation and toxin action

has received support from studies in CHO-K1 cells (*15*). When PA was bound to cells and activated by endogenous proteases, a fraction of the resulting PA_{63} was converted in a time-dependent manner to a band with mobility corresponding to that of a large oligomer (presumably a heptamer). Formation of this band was inhibited by lysosomotropic agents or conditions that inhibited endocytosis; conversely, brief treatment of cells with acidic medium caused a massive shift of PA_{63} into the band. These findings suggested that PA_{63} forms an SDS-resistant oligomer corresponding to the pore after it enters a low-pH compartment within the cell. The massive shift of PA_{63} to the high-M_r band in cells treated with acidic medium presumably reflects conversion of cell-surface PA_{63} to the pore, consistent with the permeabilization of the plasma membrane that occurs under these conditions.

When the crystallographic structure of the water-soluble PA_{63} heptamer (crystallized under slightly basic conditions in the absence of detergents) was determined, no hydrophobic surfaces were found that might interface with the hydrophobic core of a lipid bilayer (*5*). This suggested that this heptamer represented an intermediate in the pathway of pore formation, that is, a "prepore", rather than the pore itself. This observation led in turn to a model of the process by which the prepore could be transformed into the pore. This model is based on the crystallographic structure of the heptameric staphylococcal α-toxin pore, determined by Gouaux and co-workers (*16*). The α-toxin structure shows a transmembrane motif consisting of a 14-strand β-barrel formed from seven amphipathic β hairpin loops, which are in turn derived from a Gly-rich region within monomeric α-toxin. The side chains of alternating polar and nonpolar residues contact, respectively, the water-filled channel and the bilayer. Domain 2 of PA, which forms the main body of the heptamer, was found to contain a disordered amphipathic loop (D2L2) with sequence characteristics commensurate with the α-toxin model of pore formation. Strong support for this model of PA_{63} pore formation has come from recent electrophysiological studies involving single-cysteine PA mutants in D2L2 and charged thiol-reactive reagents (*17*).

In the studies presented here, we focus on the PA_{63} prepore and its conversion to the pore. We demonstrate that a pore-like form is generated in solution by treatment of the prepore with low pH or nonionic detergents. We correlate its properties with those of the pore and examine the role of D2L2 in the formation and stabilization of these heptameric structures. The results support and extend the α-toxin model of pore formation and provide a basis for further studies of the role of PA_{63} in translocation.

MATERIALS AND METHODS

Construction of PAΔD2L2. The *Escherichia coli* expression vector pET22b$^+$ (Novagen) containing the PA gene with a conservatively introduced *Sal*I site at base pair 792 was used for cloning and expression (*17*). The deletion mutant (residues 302−325, PAΔD2L2) was created via two-step recombinant PCR using appropriate primers, and a 123 bp *Sal*I−*Eco*RI fragment was subcloned back into the wild-type vector. The ligation products were transformed into *E. coli* XL1-Blue (Stratagene). The plasmid DNA was amplified, purified, and sequenced to confirm the presence of the mutation. Mutant plasmids were transformed into the *E. coli* expression host BL21(DE3).

Purification of Wild-Type and Mutant PA. Cultures were grown in Luria broth containing ampicillin at 37 °C to an OD_{600} of 0.6−1.0, and protein expression was induced by addition of isopropyl β-D-thiogalactopyranoside (1 mM) for 3 h at 30 °C. Periplasmic proteins were purified by osmotic shock by first resuspending pelleted cells in 4 mL of 20% sucrose, 5 mM EDTA, 150 μg/mL lysozyme, and 20 mM Tris-HCl (pH 8.0) per gram of cells (*18*). After incubation on ice for 40 min, 80 μL of 1 M $MgCl_2$ per gram of cells was added. The mixture was centrifuged, and the resulting supernatant containing the desired protein was concentrated and buffer exchanged [20 mM Tris (pH 8.0)] on Centriprep 30 concentration units (Amicon). The protein was then purified by anion-exchange chromatography (Q-Sepharose followed by Mono Q, Pharmacia). Proteins were purified to 90% homogeneity, as judged by SDS−PAGE.

Preparation of Nicked PA and Prepore. Nicked PA was prepared by incubating PA [20 mM Tris (pH 8.0) and 150 mM NaCl] with 0.5 μg/mL trypsin (Sigma) for 30 min at 22 °C followed by addition of 10 μg/mL soybean trypsin inhibitor (Sigma). Oligomeric PA_{63} was prepared from nicked PA (1−2 mg) by purification on a Mono Q HR 5/5 column (Pharmacia) in 20 mM diethanolamine (pH 8.6) with a 0 to 0.4 M NaCl gradient. The yield was typically 25−35% (*13*).

Polyacrylamide Gel Electrophoresis. Analysis of the PA_{63} oligomer formed in solution by SDS−PAGE was performed with a 7.5% polyacrylamide resolving gel in combination with a 4% polyacrylamide stacking region using the discontinuous gel system of Laemmli (*19*). Proteins were prepared in SDS sample buffer [0.0625 M Tris-HCl, 1.25% SDS, and 5% glycerol (pH 6.8)] at room temperature, unless otherwise indicated. Proteins were stained with either Coomassie Brilliant Blue R-250 or silver stain (Bio-Rad). Analysis of the oligomer formed in the membrane was similar, except that a 4 to 20% polyacrylamide gradient gel was used for SDS−PAGE and the PA_{63} monomeric and oligomeric bands were detected by Western blotting. Native PAGE was performed on 5% polyacrylamide gels containing 0.475 M Tris (pH 8.8) and 2 mg/mL CHAPS (*3*). Proteins were diluted in CHAPS sample buffer [50 mM CHES (pH 9.0) containing 2 mg/mL CHAPS] and electrophoresed in a running buffer of 25 mM Tris and 192 mM glycine. Gels were stained with Coomassie Brilliant Blue R-250.

Fluorescence Analyses. Mutant N306C PA was purified as described above except that 1 mM DTT was present in the purification buffers (*17*). Pyrene modification was carried out as described previously (*20*). PA_{63}-306C (2 μM) stored with 1 mM DTT was dialyzed against two changes of 20 mM Tris-HCl (pH 8.0) for 3 h. *N*-(1-Pyrene)maleimide (PM) was dissolved in *N*,*N*-dimethylformamide (DMF) at a concentration of 6 mM and the mixture slowly added to the dialyzed sample until a 30-fold molar excess of the reagent to protein was achieved. The mixture was incubated at room temperature, and after 3 h, DTT was added and the mixture dialyzed overnight. The labeling stoichiometry was 0.6−0.7 pyrene per PA_{63} monomer unit. Emission fluorescence was monitored using an Aminco SLM 500 spectroflorometer with an excitation wavelength of 342 nm.

Limited Proteolysis. PA_{63} was diluted into either 0.1 M MES-Tris (pH 8.0), 0.1 M MES-Tris (pH 7.0), or 0.1 M MES-Tris (pH 8.0) and 1.0% β-octylglucoside at 22 °C. After 1 h, chymotrypsin (20 μg/mL) was added to these samples,

and digestion was stopped after 20 min by addition of phenylmethanesulfonyl fluoride (PMSF). SDS sample buffer was added as described above, and samples were boiled for 10 min to dissociate oligomers. Digested fragments were analyzed by SDS−PAGE with an 11.25% polyacrylamide resolving gel.

In Vitro Translocation Assay. An assay for measuring PA-mediated translocation of a labeled ligand into cells has been previously described (*21*). Briefly, L6 cells were chilled to 4 °C, and then incubated with either nPA, prepore, or s-pore in buffered medium for 2 h. The cells were washed, and incubated with in vitro transcribed or translated LF_n internally labeled with [^{35}S]methionine (Promega, following kit instructions) for 2 h. After another washing step, the extracellular pH was lowered to 4.8 at 37 °C, and cells were either lysed or treated with Pronase E (a nonspecific protease) and then lysed. Proteins were precipitated from lysates by incubation with 5% trichloroacetic acid, followed by ether washing to remove detergent. Protein pellets were solubilized, and examined by SDS−PAGE followed by phosphorimager analysis. Proteins which translocated to the interior of the cells during the low-pH pulse were protected from Pronase treatment, and were visible on the gels as a radioactive band which could be quantified and compared to nonproteolyzed samples for a measure of translocation efficiency.

Protein Synthesis Inhibition Assay. Inhibition of protein synthesis as an assay of toxin translocation was performed as described previously (*22*). CHO-K1 cells were plated at a density of 4×10^4 cells per well 18 h prior to the addition of proteins. PA_{63} (2×10^{-8} M) was incubated at pH 8.0 or 5.0 for 30 min before incubation on cells (final PA_{63} concentration of 5×10^{-10} to 2×10^{-8} M) in the presence of LF_n−DTA (2×10^{-9} M). After 24 h at 37 °C, the medium was removed, and cells were washed with ice-cold PBS followed by ice-cold TCA (10%). The extent of protein synthesis was measured as the level of incorporation of radioactivity into acid-insoluble material.

Competition Assay. L6 cells were incubated at 4 °C with nPA or s-pore and various concentrations of a mutated PA in which the furin cleavage site has been altered such that the protease-specific sequence $RKKR^{167}$ was replaced with $SSSR^{167}$ (*23*). After 2 h, cells were washed twice with cold PBS and subsequently incubated with ^{35}S-labeled LF_n for 2 h at 4 °C. Cells were washed three times with cold PBS and then solubilized. Proteins were TCA precipitated from samples, and analyzed on SDS−PAGE, followed by phosphorimagery.

Rubidium Release Assay. L6 cells were plated at a density of 2×10^5 cells/well. Twelve hours after plating, medium containing $^{86}Rb^+$ (1 μCi/mL; DuPont NEN) was added to each well and the plates were incubated for an additional 12 h. Plates were chilled to 4 °C, and then incubated with either nPA, prepore, or s-pore in buffered medium for 2 h. Cells were washed to remove unbound toxin, and fresh medium was added at either pH 5.0 or 7.4. Cells were incubated for 30 min, and supernatants were removed for determination of the level of $^{86}Rb^+$ leakage using a γ counter.

RESULTS

Effects of pH and Detergents on the Prepore. PA_{63} purified under mildly basic conditions (pH 8.0−9.0) was negatively stained and confirmed by electron microscopy to be in the form of ring-shaped heptamers. For simplicity, we refer to this soluble, high-pH form of the PA_{63} heptamer as the prepore. The protein migrated as a single band on PAGE under nondenaturing conditions (pH 8.0 in the presence of CHAPS) and exhibited very low electrophoretic mobility relative to that of PA or trypsin-nicked PA (*3*) (Figure 2a). No monomeric PA_{63} or oligomers other than the heptamer were observed. The monomer−heptamer equilibrium is therefore greatly in favor of the heptamer. After incubation

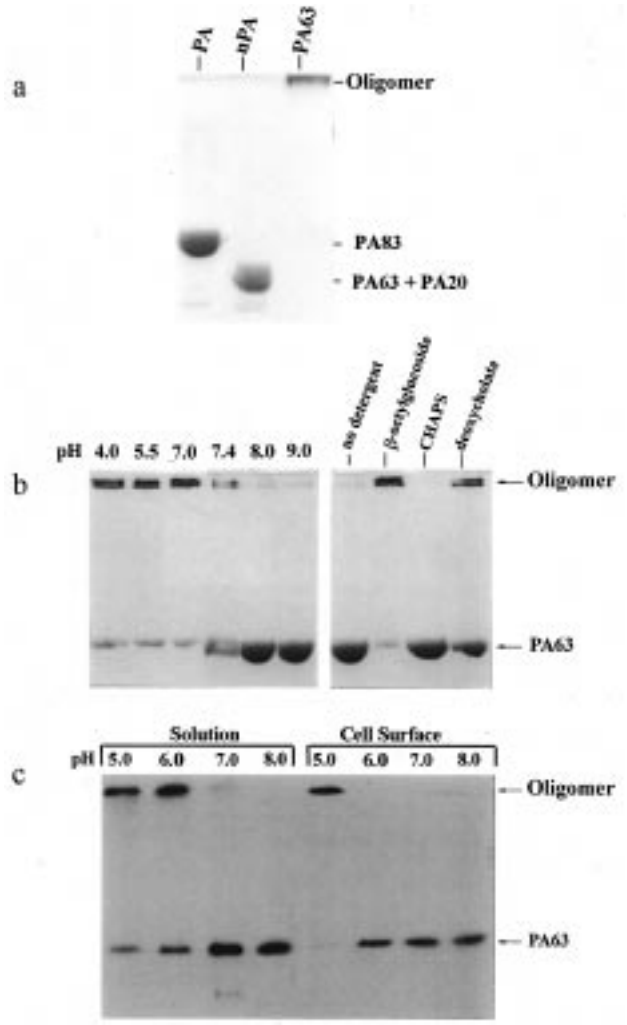

FIGURE 2: PAGE analysis of PA_{63}. (a) Twenty-five microliter samples of PA (0.15 mg/mL), nPA (0.15 mg/mL), and PA_{63} (0.10 mg/mL) in sample buffer containing 50 mM CHES (pH 9.0) and 2 mg/mL CHAPS were run on a nondenaturing 5% polyacrylamide gel followed by staining with Coomassie Blue. (b) PA_{63} [20 mM ethanolamine (pH 9.0)] was diluted 5-fold to 0.1 mg/mL at the desired pH (citrate, pH 4.0; MES, pH 5.5 and 7.0; HEPES, pH 7.4; Tris, pH 8.0; and ethanolamine, pH 9.0) or at pH 8.0 (20 mM Tris) with the indicated detergent (1% β-OG, 0.6% DOC, or 0.5% CHAPS). Samples were diluted in SDS sample buffer, run on 7.5% polyacrylamide gels containing SDS, and stained with Coomassie blue. (c) PA_{63} (2×10^{-8} M) was incubated with L6 cells for 30 min on ice. The cells were washed with PBS and incubated in the appropriate buffer (MES-gluconate, pH 5.0; MES, pH 6.0 and 7.0; and Tris, pH 8.0) on ice for an additional 15 min. Cells were solubilized in SDS sample buffer with 1% Triton, and the amount of SDS-resistant oligomer was determined by SDS−PAGE and Western blot analysis. Control solution samples were prepared simultaneously by diluting stock PA_{63} (2×10^{-8} M) 10-fold into appropriate buffers and were processed in a manner identical to that of cellular samples.

with 1.25% SDS at room temperature, the preparation gave a strong 63 kDa band on SDS−PAGE together with traces of a high-M_r band (Figure 2b). This indicates that the prepore dissociates to monomers in SDS, even at room temperature. We believe the faint high-M_r band represents traces of the SDS-resistant pore-like form described below.[2]

We incubated samples of prepore for 1 h at room temperature in solutions buffered at pH values from 4.0 to 9.0 and then treated them with SDS (1.25%) and analyzed them by SDS−PAGE (Figure 2b). In samples incubated at pH ≤7.0, a large fraction of the protein was converted to an SDS-resistant high-M_r form which comigrated with that observed in PA-treated cells. This shows that neutral-to-acidic conditions trigger conversion of the prepore to a pore-like form in solution. (To avoid confusion, we have designated this solution form the s-pore and that formed in membranes the m-pore.) We compared the pH dependence of conversion of prepore to s-pore in solution with conversion of prepore bound to the surface of L6 cells to m-pore. As shown in Figure 2c, the threshold for conversion to m-pore was significantly lower (∼1 pH unit) than that for conversion to s-pore under identical conditions, implying a greater conformational constraint in the membrane-bound state.

Also, of note is the fact that the maximum pH at which the s-pore was formed in solution was lower in Figure 2c than in Figure 2b. This can be explained by the experiment whose results are depicted in Figure 2c being carried out over less time (15 min) and at a lower temperature (4 °C) to minimize endocytosis. Conversion to the m-pore was almost quantitative at pH 5, whereas conversion to s-pore was never complete, for unknown reasons. Little or no s-pore was generated when trypsin-nicked PA (nPA) was treated at low pH, consistent with the notion that the prepore is an essential intermediate in low-pH-dependent pore formation. However, when nPA was bound and incubated on the cell surface, the conversion to m-pore induced by acidic pH was the same as for prepore. This suggests that nPA converts to a species similar to that of prepore bound to the cell surface.

Transition of the prepore to the s-pore was not reversed when samples of PA_{63} that had been treated at pH 7.0 were diluted into pH 8.0 buffer before SDS−PAGE. However, both s- and m-pore dissociated to monomers when treated at 100 °C for 10 min in the presence of SDS. This confirms that noncovalent interactions are responsible for stability of these forms. Addition of SDS to prepore at pH 8.0 before lowering the pH blocked formation of the SDS-resistant oligomer. Conversion to s-pore was not significantly affected by the concentration of PA_{63} (between 0.05 and 1 mg/mL), the concentration of NaCl (up to 1 M), or the addition of $CaCl_2$ (1 mM) or EDTA (0.5 mM). Two closely spaced s-pore bands were seen in most experiments, suggesting the existence of more than one conformational state.

Addition of β-octylglucoside (β-OG) to 1% induced rapid conversion of the prepore to the s-pore, even at pH 8.0 (Figure 2b). Deoxycholate (DOC) at 0.6% was less effective at inducing conversion, and CHAPS (0.5%) was inactive. DOC has also been shown to induce formation of an SDS-resistant heptamer of α-toxin (*24*). The s-pore was less soluble than the prepore, as shown by its ability to be pelleted when centrifuged at 15000*g* for 20 min. β-OG or DOC maintained the protein in a soluble state.

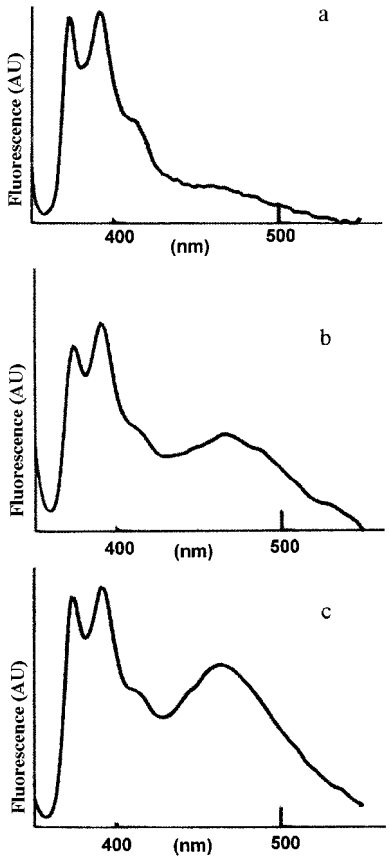

FIGURE 3: Excimer formation by pyrene-labeled N306C PA_{63}. Pyrene-modified N306C PA_{63} was diluted to 0.1 mg/mL in buffers containing (a) 50 mM MES-Tris (pH 8.0), (b) 50 mM MES-Tris (pH 7.0), or (c) 20 mM Tris (pH 8.0) and 1.0% β-octylglucoside. Emission fluorescence spectra (375−500 nm) were recorded with an excitation wavelength of 342 nm.

Probing the State of D2L2 by Fluorescence. We labeled a site in the D2L2 loop (N306C) with pyrene and monitored pyrene excimer formation under various conditions as a means of confirming that a major conformational transition of this loop occurs during pore formation. The pyrene excimer is an excited-state complex with a broad band in its emission spectrum at a λ_{max} of ≅470. Formation of the pyrene excimer is dependent on the close approach of pyrene molecules (∼10 Å) (*25*), and excimer formation is often used to detect conformational changes that alter distances between cysteine-bound pyrenes in proteins (*20*). In the prepore, pyrene groups within D2L2 would be expected to be too far apart to permit excimer formation, but relocation of D2L2 to the base of the heptamer, as required for β-barrel formation (*5*), should permit direct contact of the loops from the various monomers. In the absence of detergents, formation of a perfect β-barrel in solution would not be expected, but the relocated pyrene-containing loops should nonetheless be free to interact in a disordered or partially ordered state.

Prepore containing the N306C mutation was reacted with pyrene maleimide, and the emission spectrum was recorded, with excitation at 342 nm. As shown in Figure 3a, the pyrene emission spectrum of the derivatized prepore at pH 8.0 exhibited only weak emission at 470 nm, but a prominent

[2] Slow conversion to the pore-like form may occur in solution even at pH ≥8. Alternatively, these traces may have formed at the air−water interface or another surface in contact with the solution.

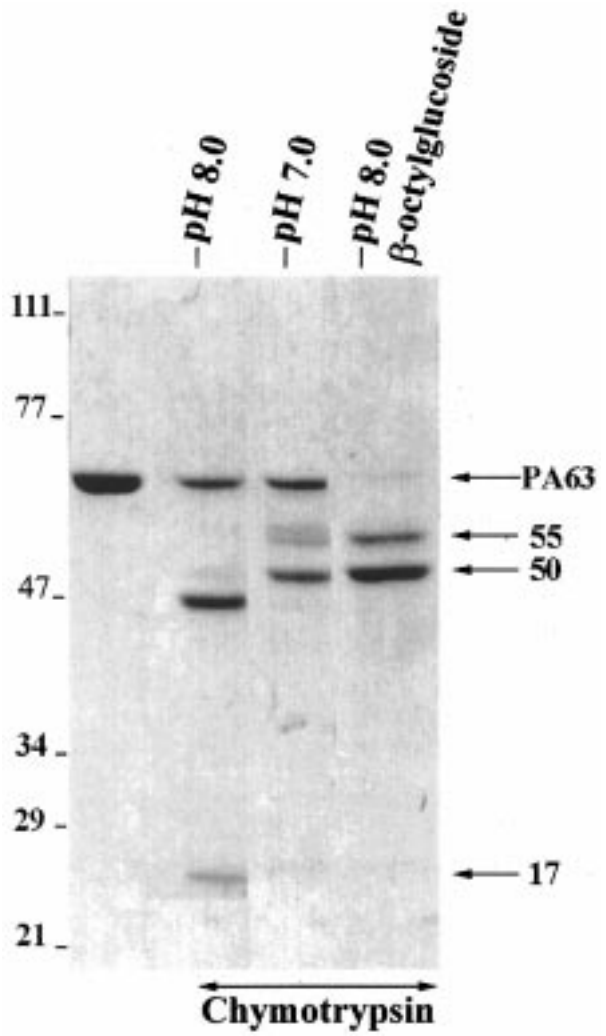

FIGURE 4: Chymotryptic digestion of prepore and s-pore. PA_{63} was diluted into either 20 mM MES-Tris (pH 8.0), 20 mM MES-Tris (pH 7.0), or 20 mM MES-Tris (pH 8.0) buffer containing 1.0% β-OG and incubated for 1 h at 22 °C. Samples were then digested with chymotrypsin (20 μg/mL) at pH 8.0 for 20 min before stopping the reaction with PMSF. SDS sample buffer was added, and the samples were treated at 100 °C for 10 min and analyzed by SDS−PAGE on 11.25% polyacrylamide gels.

peak with a λ_{max} of ≅470 appeared upon incubation of the sample at pH 7.0 (Figure 3b). Incubation of the derivatized protein in 1.0% β-OG at pH 8.0 generated even stronger excimer emission (Figure 3c). Thus, two different conditions known to induce the prepore to convert to the s-pore also induced excimer formation, supporting the proposed role of D2L2 in prepore-to-pore conversion.

Probing the State of D2L2 by Proteolysis. Limited digestion with chymotrypsin has been shown to effect specific cleavage of native PA between F314 and D315 within the D2L2 loop, generating 47 and 37 kDa fragments (*26*). This is consistent with the fact that D2L2 was found to be disordered and in an exposed location in the crystallographic structure of native PA. To determine whether this chymotrypsin site within D2L2 is accessible in the prepore and s-pore forms of PA_{63}, we incubated purified PA_{63} at pH 7.0 or 8.0 (with or without β-OG and DOC) for 1 h at room temperature, digested the samples with chymotrypsin (20 μg/mL) at pH 8.0, treated them for 10 min at 100 °C, and analyzed them by SDS−PAGE (Figure 4).

Prepore incubated with chymotrypsin at pH 8.0 yielded 47 and 17 kDa fragments, consistent with a single cleavage after residue F314 (Figure 4). This indicated that the state of D2L2 in the prepore is largely unchanged from that in native PA. In contrast, the sample incubated at pH 7.0 yielded chymotryptic fragments, all with a mass of >47 kDa. This indicates that the F314 site is obscured in the s-pore and that other sites become exposed during prepore-to-pore conversion. N-Terminal sequencing of these fragments showed that they retained the N-terminus of PA_{63} (beginning with K167). From this fact and the sizes of the major fragments (approximately 50 and 55 kDa), we estimate that the sites of chymotryptic cleavage in the pore are within domain 4 (residues 596−735) and the C-terminal region of domain 3 (residues 488−595). Chymotryptic digestion of PA_{63} treated with 0.6% DOC or 1.0% β-OG at pH 8.0 gave the same digestion pattern as s-pore formed in the absence of detergents, demonstrating the similarity of conformational changes induced by these detergents to those induced by acidic pH.

Effects of Deleting D2L2. To probe the contribution of D2L2 to the stability of the s-pore, we created a mutant form of PA (PAΔD2L2) in which this loop (residues 302−325) was deleted. Trypsin cleaved PAΔD2L2 specifically at the furin site, as judged by the sizes of the peptide fragments (20 and 60 kDa). The larger fragment, PA_{60} (corresponding to PA_{63} from wild-type PA), could be purified by the same protocol that was used for purification of PA_{63}, and was inactive in assays for formation of membrane channels or translocation of A moieties to the cytosol of cells.

PA_{60} self-associated to form an SDS-labile heptamer similar to the PA_{63} prepore, as shown by PAGE under nondenaturing conditions and electron microscopy. When PA_{60} was incubated at pH 7.0, a high-M_r SDS-resistant oligomer was generated, similar to that seen with wild-type PA_{63} (Figure 5). Surprisingly, β-OG and DOC also induced transition of PA_{60} prepore to the s-pore form, implying interactions of the detergents with a region of the protein other than D2L2. The fact that the conformational change of PA_{60} at pH 7.0 is analogous to that of PA_{63} is supported by the change in the chymotryptic digestion pattern. PA_{60} was not cleaved by chymotrypsin at pH 8.0, consistent with the absence of the D2L2 site, but after incubation at pH 7.0, it gave a cleavage pattern similar to that of the wild-type s-pore.

The fact that PA_{60} can be converted to a high-M_r form that survives exposure to SDS at room temperature implies that strong subunit−subunit interactions between the globular parts of domain 2 are retained. Also, it shows that resistance to SDS does not depend primarily on interactions of D2L2 loops. The D2L2 deletion does somewhat diminish the overall stability, however, as the PA_{60} s-pore dissociated more rapidly than the wild-type s-pore in SDS at 100 °C. The fact that the PA_{60} prepore converts to an SDS-stable form at pH 7 also implies that D2L2 is not crucial for pH sensing.

Functional Properties of the Prepore and s-Pore. The s-pore form of PA_{63} was prepared in solution at a low concentration (2×10^{-8} M) to minimize aggregation before testing for translocation activity on cells. To assess delivery of an enzymic ligand to the cytosol, we employed a fusion protein consisting of LF_n, the N-terminal PA_{63}-binding 255-

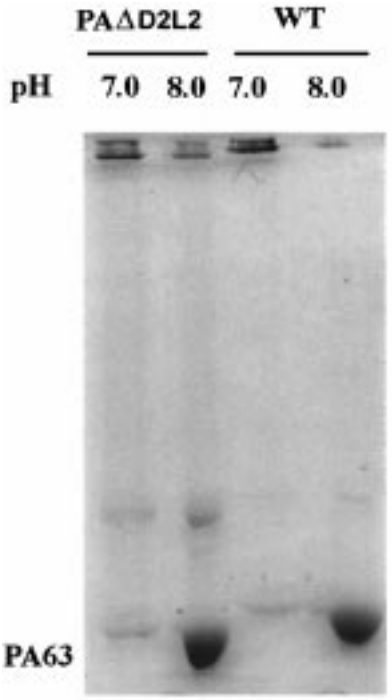

FIGURE 5: PAGE analysis of prepore and s-pore forms of PAΔD2L2. The PA_{63} form of wild-type PA and the PA_{60} form of PAΔD2L2 [20 mM ethanolamine (pH 9.0)] were diluted 5-fold to 0.1 mg/mL in MES (pH 7.0) or Tris (pH 8.0). Samples were diluted in SDS sample buffer, run on 7.5% polyacrylamide gels containing SDS, and stained with Coomassie blue.

residue domain of LF, fused to the A chain of diphtheria toxin (DTA). DTA inhibits protein synthesis by catalyzing the ADP ribosylation of elongation factor 2. As shown in Figure 6a, the prepore was almost as active as nPA in delivering LF_n−DTA, whereas the s-pore was entirely inactive at concentrations as high as 20 nM. We also measured the ability of PA derivatives bound to the cell surface to translocate radiolabeled LF_n across the plasma membrane upon treatment with low-pH medium (*21*). Cell-associated s-pore bound [^{35}S]LF_n as effectively as the prepore and nPA (Figure 6b), but it was inactive in translocation, in contrast to the prepore, which was as active as nPA (Figure 6b). In addition, s-pore formed after addition of 1.0% β-octylglucoside was also unable to translocate LF_n in either assay.

To determine whether binding of s-pore to the cell surface was receptor-dependent or nonspecific, we measured the ability of a mutant form of PA, PA-$SSSR^{167}$, to compete for binding of nicked PA or s-pore to L6 cells. PA-$SSSR^{167}$ (*23*) contains mutations in the furin site ($RKKR^{167}$) that prevent proteolytic activation, thereby blocking oligomerization and ligand binding. Cells were treated with nPA or s-pore in the presence of the competitor PA-$SSSR^{167}$ (20−400 pM), and the amount of bound PA_{63} or s-pore was assayed by measuring the level of binding of labeled LF_n. As shown in Figure 7, PA-$SSSR^{167}$ clearly inhibited binding of s-pore, although its inhibition of nicked PA was somewhat more efficient. We conclude that at least a substantial fraction of the cell-associated s-pore was bound via the PA receptor.

The foregoing results suggested that the inactivity of the s-pore in translocation results from an inability to insert into membranes. We therefore tested nPA, prepore, and s-pore for ability to release $^{86}Rb^+$ from L6 cells preloaded with this

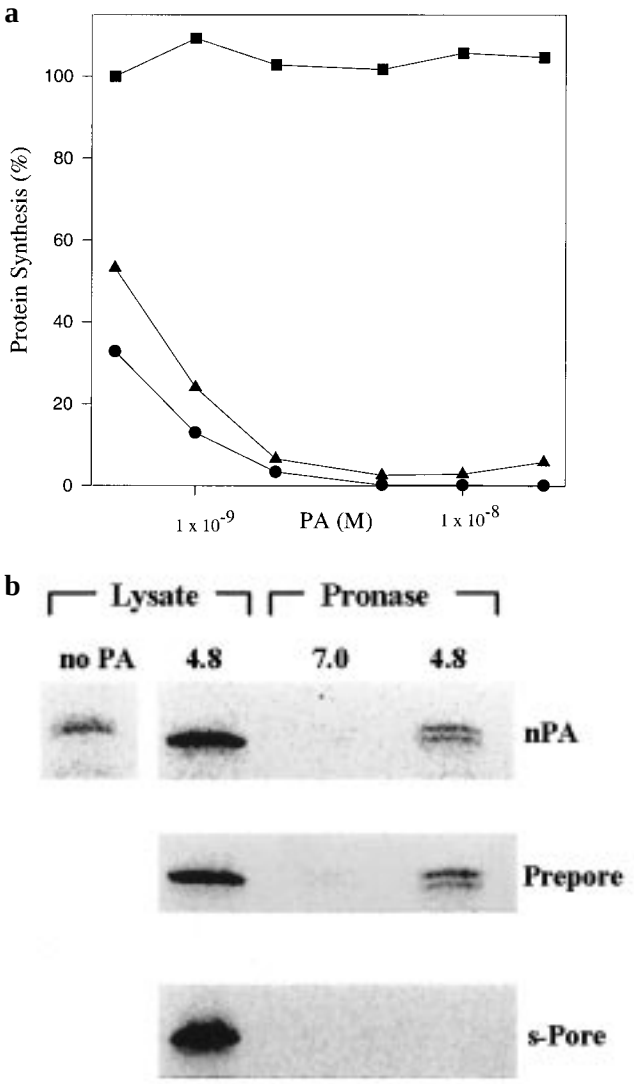

FIGURE 6: S-Pore does not translocate LF_n−DTA to the cytosol. (a) The s-pore was prepared by first incubating PA_{63} for 30 min in 0.1 M MES-Tris (pH 5.0). Samples of nicked PA (●), prepore (▲), and s-pore (■) were added to CHO/K-1 cells over a concentration range of 5×10^{-10} to 2×10^{-8} M in the presence of 2×10^{-9} M LF_n−DTA. After 24 h at 37 °C, the extent of protein synthesis was measured. Results are expressed as the percentage of protein synthesis in the absence of added proteins. (b) L6 cells were incubated with nPA, prepore, or s-pore for 2 h at 4 °C, washed, and incubated further with radiolabeled LF_n for 2 h at 4 °C. Cells were then either lysed directly (total bound) or briefly incubated at 37 °C with acidic or neutral buffer and subsequently treated with Pronase (translocated). Finally, cells were lysed, the nuclei removed, and the proteins TCA precipitated from the cell lysate and analyzed by SDS−PAGE followed by fluorography.

marker (*27*). As shown in Figure 8, cell surface-bound prepore and nPA mediated release of $^{86}Rb^+$ upon incubation at pH 5.0 (Figure 8), whereas s-pore did not. The s-pore therefore represents an abortive form, whose conformation precludes membrane insertion or production of a functional channel.

DISCUSSION

A detailed understanding of how an AB toxin translocates its enzymic moiety across a membrane is perhaps closest at hand in those toxins that carry their own membrane translocation machinery, that is, those in which the B moiety is

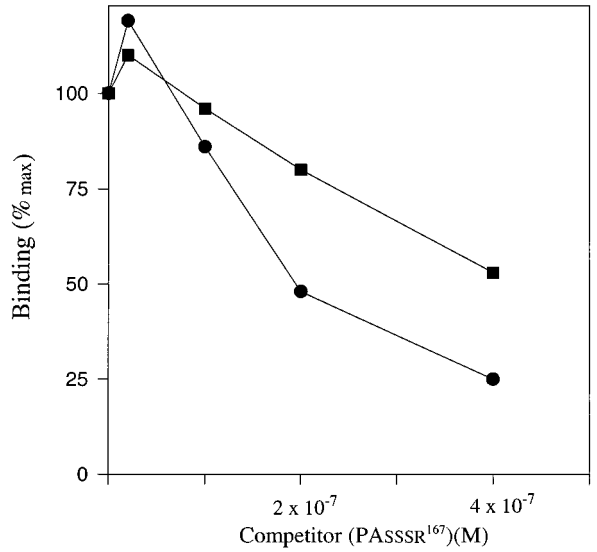

FIGURE 7: S-Pore binds specifically to cell receptors. L6 cells were first exposed to either nPA (●) or s-pore (■) (prepared as described in the legend of Figure 6) and the specified quantity of competitor PA-$SSSR^{167}$ at 4 °C for 2 h, followed by washing with PBS. A second incubation with labeled LF_n followed, again at 4 °C to prevent endocytosis, and the cells were washed. Cells were lysed; proteins were precipitated and run on gels, and the radioactive LF_n band was quantified by phosphorimagery. The *y*-axis is the percentage of binding in the absence of competitor.

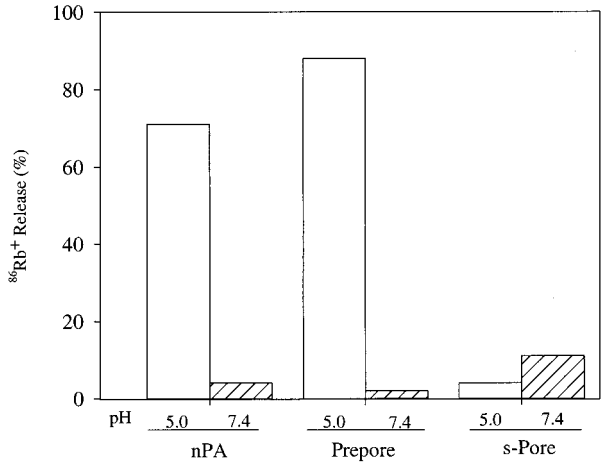

FIGURE 8: s-Pore is unable to form pores in the plasma membrane of L6 cells. L6 cells loaded with $^{86}Rb^+$ were incubated for 2 h at 4 °C with either nPA, prepore, or s-pore. To determine the extent of $^{86}Rb^+$ release, cells were washed, medium (pH 7.4 or 5.0) was added, and after 30 min the cellular supernatant was counted. Spontaneous release was determined for cells in the absence of PA.

capable of converting to an integral membrane form and generating a pore. Two major strategies of pore formation by AB toxins are known. (i) In diphtheria, botulinum, and tetanus toxins, an α-helical domain serves as the insertion element and forms a pore that may, at least in the case of diphtheria toxin, be monomeric (*28*). (ii) In anthrax toxin, and presumably other binary toxins, the B moiety generates an oligomeric ring-shaped pore in which the transmembrane motif is a *β*-barrel.

In anthrax toxin, it now seems certain that pore formation proceeds via an intermediate corresponding to the PA_{63} heptamer. Prepore assembled in solution and then bound to cells was active in translocating PA_{63} ligands in both a cell-surface translocation assay and an assay depending on the normal endocytic pathway. Also, it was able to form ion-conductive pores in the plasma membrane, as determined by ion leakage experiments. Prepore intermediates have been identified in other pore-forming toxins, such as α-hemolysin, and proteolytic cleavage also serves to potentiate the protein for pore formation in some of them (*29*).

Earlier, it was shown that cell-associated PA_{63} was triggered to form an SDS-resistant oligomer by acidic pH (pH ∼5), a condition known to promote pore formation and A moiety translocation (*12*). However, pore formation in planar lipid bilayers was found to occur even at pH 7 (*13*), which correlates more closely with the pH dependence of the conversion of prepore to pore in solution. In a direct test of the pH dependence of prepore-to-pore conversion in solution versus conversion on L6 cells, we found that the latter required a significantly lower pH, indicating a greater energy barrier to the conversion in the membrane-bound state. Examination of the crystallographic structure of the prepore has revealed that relocation of the D2L2 loop to the base of the structure necessitates movement of domain 4 (C. Petosa, personal communication), and it may be that this movement is constrained by the interaction of domain 4 with the PA receptor.

The pH sensing mechanism for the conformational change to the pore has not been examined, but the fact that the conversion occurs at neutral pH in solution strongly suggests the involvement of histidines, of which there are nine in PA_{63}. Five of them are part of a cluster within D2L2 (His-304 and His-310) or proximal to the loop (His-263, -299, and -336). The fact that D2L2 could be removed from PA_{63} without affecting the pH at which the prepore is converted to pore in solution suggests this loop does not have a direct role in the pH sensing mechanism (*5*).

β-Octylglucoside, and to a lesser extent deoxycholate, also induced prepore-to-pore transition of PA_{63} and increased the solubility of the pore form. These detergents presumably mimic membrane conditions and interact primarily with D2L2, lowering the activation barrier to formation of a *β*-barrel. The fact that *β*-octylglucoside also triggered conversion of D2L2-deleted PA_{63} to the SDS-resistant state indicates, however, that such detergents also interact with other sites within the protein. One possible site is the 2*β*3−2*β*4 loop, which is adjacent to a segment (the 2*β*3 strand) that is believed to undergo a rearrangement during pore formation. This loop changes from an ordered state in crystals grown at pH 7.5 to a disordered state in crystals grown at pH 6.0, and contains apolar residues (W346, M350, and L352) that may interact with the bilayer (*5*).

The finding that conversion to the SDS-resistant pore induced by acidic pH was not reversed under basic conditions supports the conclusions from membrane bilayer experiments that pore formation is an essentially irreversible step (*13*).

Several of our results support the hypothesis based on the crystallographic structure of the prepore that the D2L2 loops undergo a major conformational rearrangement during pore formation.

(i) Mutant PA lacking D2L2 was incapable of forming pores and mediating translocation, although its abilities to be proteolytically activated, to self-assemble to the prepore state, and to convert to an SDS-resistant oligomer were unimpaired.

(ii) The only accessible chymotrypsin site in PA_{63}, which lies within D2L2, became inaccessible when the prepore underwent transition to the pore-like state in solution in response to acidic pH or detergents. Occlusion of the chymotrypsin site would be expected if β-barrel formation were to occur in solution, as is likely in the presence of detergents. In the absence of detergents, it is more likely that the D2L2 loops interact to form an aberrant structure in which the hydrophobic side chains, including F313 and F314, which flank the chymotrypsin cleavage site, are occluded.

(iii) Pyrene groups linked to a cysteine substituted for Asp-306 generated a strong excimer band after transition to the s-pore. The virtual absence of an excimer band in the prepore is consistent with the location of the D2L2 loops in this form, on the periphery of domain 2. The strong band generated after lowering the pH or adding β-octylglucoside indicates a conformational rearrangement that allows intimate interactions of the D2L2 loops.

Major rearrangements also occur in the globular elements of the prepore during conversion to the pore. Mutant prepore lacking D2L2 retained the ability to adopt an SDS-resistant conformation, implying that stabilizing conformational rearrangements occurred in domains 1 and 2 and/or in domains 3 and 4. For the D2L2 loops to assemble into a β-barrel on the heptamer axis, the Greek-key motif formed by the first four strands of domain 2 ($2\beta1-2\beta4$) has been proposed to unfold (*5*). Strands $2\beta2$ and $2\beta3$ (which flank D2L2) peel away from the domain according to this model, allowing the loop to relocate to the base of the heptamer. This implies a major conformational rearrangement of the globular portion of domain 2 that may contribute to the SDS resistance. The fact that the s-pore generated from the D2L2 mutant dissociates more readily in SDS at 100 °C than the wild-type form implies that interactions between these loops also contribute to the stability of the pore. Conversion to the pore exposes new chymotrypsin sites within domain 4 or the C-terminal part of domain 3, indicating conformational changes in one or both of these domains as well.

The results presented here provide insight into the structural changes that drive toxin translocation but do not indicate that the s-pore is a step in the intoxication pathway. The conformational changes in conversion of the prepore to the s-pore did not impair the protein's ability to bind receptors (showing that domain 4 retains functionality) or PA_{63} ligands (indicating functionality of subdomain 1b, where ligand binding is believed to occur). The protein's ability to mediate translocation or permeate membranes was ablated, however. Thus, conversion of prepore to the s-pore involves an irreversible step that leaves the oligomer unable to insert into membranes and/or to generate a transmembrane β-barrel. This suggests that insertion competence depends on D2L2 remaining in its "poised" state in the prepore before membrane binding. The prepore is thus a spring-loaded structure that is capable of forming a pore when triggering occurs after it is bound to a membrane but that converts to an abortive structure when triggering occurs in solution. This implies that anthrax toxin has evolved to self-assemble with PA in the receptor-bound form, such that the prepore only forms in close proximity to a membrane.

The means by which the prepore-to-pore conversion described here fits into the overall mechanism of translocation of anthrax toxin's enzymic moieties across the endosomal membrane remains to be determined. One possibility is that pH-induced pore formation precedes translocation and that the pore plays an essentially passive role. In its simplest form, this model assumes that the ability of enzymic moieties to be translocated is determined by their capacity to bind to the prepore and to unfold sufficiently under conditions of translocation (*21*) (the lumen of the β barrel is ~16 Å in diameter). A second possibility is that the prepore-to-pore conversion, besides forming a passageway, actively mediates other steps in the translocation process. For example, it may be that the conformational rearrangements in the globular extramembranous domains of PA_{63} facilitate the unfolding of bound EF or LF as a prelude to their translocation. Neither of these models excludes the possibility that other, cellular factors may participate in translocation. The results reported here provide a foundation for studies of such models.

ACKNOWLEDGMENT

We thank Kate Beauregard for the mutant PA strain PA-SSSR[167].

REFERENCES

1. Zhan, H., Elliot, J., Shen, W., Finkelstein, A., and Collier, R. (1999) *J. Membr. Biol. 167*, 173−81.
2. O'Keefe, D. (1992) *Arch. Biochem. Biophys. 296*, 678−84.
3. Singh, Y., Klimpel, K. R., Arora, N., Sharma, M., and Leppla, S. H. (1994) *J. Biol. Chem. 269*, 29039−46.
4. Leppla, S. H. (1991) in *Sourcebook of bacterial protein toxins* (Aloug, J., Ed.) pp 277−302, Academic Press, New York.
5. Petosa, C., Collier, R. J., Klimpel, K. R., Leppla, S. H., and Liddington, R. C. (1997) *Nature 385*, 833−8.
6. Escuyer, V., and Collier, R. J. (1991) *Infect. Immun. 59*, 3381−6.
7. Klimpel, K. R., Arora, N., and Leppla, S. H. (1994) *Mol. Microbiol. 13*, 1093−100.
8. Friedlander, A. M. (1986) *J. Biol. Chem. 261*, 7123−6.
9. Gordon, V. M., Leppla, S. H., and Hewlett, E. L. (1988) *Infect. Immun. 56*, 1066−9.
10. Leppla, S. H. (1982) *Proc. Natl. Acad. Aci. U.S.A. 79*, 3162−6.
11. Duesbery, N. S., Webb, C. P., Leppla, S. H., Gordon, V. M., Klimpel, K. R., Copeland, T. D., Ahn, N. G., Oskarsson, M. K., Fukasawa, K., Paull, K. D., and Vande Woude, G. F. (1998) *Science 280*, 734−7.
12. Milne, J. C., Furlong, D., Hanna, P. C., Wall, J. S., and Collier, R. J. (1994) *J. Biol. Chem. 269*, 20607−12.
13. Blaustein, R. O., Koehler, T. M., Collier, R. J., and Finkelstein, A. (1989) *Proc. Natl. Acad. Sci. U.S.A. 86*, 2209−13.
14. Koehler, T. M., and Collier, R. J. (1991) *Mol. Microbiol. 5*, 1501−6.
15. Milne, J. C., and Collier, R. J. (1993) *Mol. Microbiol. 10*, 647−53.
16. Song, L., Hobaugh, M. R., Shustak, C., Cheley, S., Bayley, H., and Gouax, J. E. (1996) *Science 274*, 1859−66.
17. Benson, E. L., Huynh, P. D., Finkelstein, A., and Collier, R. J. (1998) *Biochemistry 37*, 3941−8.
18. Ausubel, F. M., Brent, R., Kingston, R. E., Moore, D. D., Seidman, J. G., Smith, J. A., and Struhl, K. (1993) *Current Protocols in Molecular Biology*, John Wiley and Sons, Inc., New York.
19. Laemmli, U. K. (1970) *Nature 227*, 680−5.
20. Zhan, H., Choe, S., Huynh, P., Finkelstein, A., Eisenberg, D., and Collier, R. J. (1994) *Biochemistry 33*, 11254−63.
21. Wesche, J., Elliott, J. L., Falnes, P. Ø., Olsnes, S., and Collier, R. J. (1998) *Biochemistry 37*, 15737−46.
22. Blanke, S. R., Milne, J. C., Benson, E. L., and Collier, R. J. (1996) *Proc. Natl. Acad. Sci. U.S.A. 93*, 8437−42.

23. Ballard, J. D., Doling, A. M., Beauregard, K., Collier, R. J., and Starnbach, M. N. (1998) *Infect. Immun. 66*, 615−9.
24. Bhakdi, S., Fussle, R., and Tranum-Jensen, J. (1981) *Proc. Natl. Acad. Sci. U.S.A. 78*, 5475−9.
25. Lerhrer, S. S. (1995) in *Subcellular Biochemistry* (Roy, S., Ed.) pp 115−33, Plenum Press, New York.
26. Novak, J. M., Stein, M.-P., Little, S. F., Leppla, S. H., and Friedlander, A. M. (1992) *J. Biol. Chem. 267*, 17186−93.
27. Milne, J. C., Blanke, S. R., Hanna, P. C., and Collier, R. J. (1995) *Mol. Microbiol. 15*, 661−6.
28. Huynh, P., Cui, C., Oh, K., Collier, R., and Finkelstein, A. (1997) *J. Gen. Physiol. 110*, 229−42.
29. Valeva, A., Weisser, A., Walker, B., Kehoe, M., Bayley, H., Bhakdi, S., and Palmer, M. (1996) *EMBO J. 15*, 1857−64.

BI990792D